Numerical Simulation and Experimental Research of the Hydrostatic Extrusion Process of Pure Tungsten

Shengqiang Du, Kaijun Hong, Xiang Zan, Ping Li, Laima Luo, Yang Yu and Yucheng Wu

Abstract A finite element model (FEM) of the hydrostatic extrusion (HE) process with pressure load model is established in this paper. On this basis, the hot hydrostatic extrusion process of sintered pure tungsten under different temperatures (T), extrusion ratios (R) and die angles (α) are simulated by introducing the Johnson-Cook constitutive relation for material flowing behavior. The simulation results show that there is a negative correlation between the extrusion pressure (P) and T, a positive correlation between P and lnR. And during the increase of the α value, the P value decreases first and then increases. The die angle corresponding to the minimum P is different under different extrusion ratio. Furthermore, a

S. Du · X. Zan (✉) · P. Li · L. Luo · Y. Wu
School of Materials Science and Engineering, Hefei University of Technology, Hefei 230009, China
e-mail: zanx@hfut.edu.cn

S. Du
e-mail: 15255150652@163.com

P. Li
e-mail: li_ping@hfut.edu.cn

L. Luo
e-mail: luolaima@126.com

Y. Wu
e-mail: ycwu@hfut.edu.cn

K. Hong · P. Li · Y. Wu
Institute of Industry and Equipment Technology, Hefei University of Technology, Hefei 230009, China
e-mail: 2016170186@mail.hfut.edu.cn

X. Zan · L. Luo · Y. Wu
National–Local Joint Engineering Research Centre of Nonferrous Metals and Processing Technology, Hefei 230009, China

Y. Yu
School of Materials Science and Engineering, Harbin Institute of Technology—Weihai, Weihai 264209, China
e-mail: hityyang@hit.edu.cn

Y. Han (ed.), *Advances in Energy and Environmental Materials*,
Springer Proceedings in Energy, https://doi.org/10.1007/978-981-13-0158-2_19

tendency of internal cracking during the process can be found when the R value is relatively small. Based on the simulation results, the experiment of hot hydrostatic extrusion of sintered pure tungsten is carried out. The microhardness, microstructure and mechanical properties of the tungsten before and after the process are investigated. The results show that after the hot hydrostatic extrusion, the grain size of the tungsten is subdivided, the hardness is improved obviously and the mechanical properties is remarkable.

Keywords Pure tungsten · Hydrostatic extrusion · Finite element analysis
Microhardness · Microstructure · Mechanical properties

Introduction

Pure tungsten has the advantages of high melting point, high thermal conductivity, low sputtering rate and low vapor pressure etc., and is considered to be the primary candidate as plasma facing materials (PFM) used in the future nuclear fusion heap [1–4]. The ITER organization decided to develop the full tungsten divertor in 2011 [5, 6]. But tungsten materials have the disadvantages of the low intergranular combination degree, brittleness in low temperature or under irradiation, and high ductile-brittle transition temperature, leading to the great limitation of its application [7]. The plastic deformation process is an effective method to refine the tungsten grain size, increasing the density, so that the microstructure and the thermal conductivity can be improved. Furthermore, the ductile-brittle transition temperature can be reduced and the high temperature mechanical properties, and anti-radiation brittlement performance will be improved, either. Hydrostatic extrusion is a severe plastic deformation method (SPD) that forces the material to deform by hydrostatic pressure. During the forming process, the material is under hydrostatic compressive state which could greatly improve the formability of the material. It is one of the most effective methods to fabricate the refractory materials such as tungsten [8–10].

In recent years, finite element analysis (FEA) has gradually become an effective means to study the hydrostatic extrusion of tungsten. Through the research, it was found that there were obvious differences in the stress distribution under different extrusion temperature, extrusion ratio and die angle. Inappropriate selection of process parameters may lead to defects such as surface cracks and internal cracks [11]. Meanwhile, the temperature (T), the extrusion ratio (R) and the die angle (2α) were the three of most important parameters affecting the extrusion pressure [8, 12, 13]. Moreover, the shape of die contours could affect the extrusion pressure and the stress distribution to some extent [14]. By comparing the results of numerical simulation and corresponding experiments, some errors could be found, which were mainly caused by geometric errors, experimental statistical errors and too idealization and simplification of traditional finite element models [15].

So far, all FEA studies on the hydrostatic extrusion of pure tungsten were based on the simplified hydrostatic extrusion model with displacement loads and rigid

restraints, which did not reflect the hydrostatic pressure feature. In the present study, the FEA under hydrostatic pressure loads is designed and the constitutive relation of pure tungsten is introduced. The effect of parameter R and α on the hydrostatic extrusion under different temperatures is studied. Additionally, the hydraulic extrusion experiment is completed under the guidance of the simulation results, the microhardness, microstructure and mechanical properties of sintered pure tungsten before and after the extrusion are contrasted.

FEA Methods and Materials

Hydrostatic extrusion is a SPD method that forces the material to deform by means of liquid pressure (Fig. 1a). In the HE process, the billet is tapered to match the die geometry, the gap between the billet and the container is filled with pressure medium surrounding the billet and conveys the extrusion force of the moving punch onto it and the pressure medium is forced by its inherent pressure into the gap between the die and the billet generating excellent lubrication on the contact surface [16, 17]. Hydrostatic pressure and good lubrication conditions are beneficial for plastic deformation process of brittle materials, difficult-to-deformation materials [18]. While, in the conventional extrusion, the billet is pressed by the punch directly and so deformed (Fig. 1b).

Currently, displacement loads are used in almost all of the hydrostatic extrusion simulations [19, 20]. The displacement loads with even speed is directly applied on the upper surface of the billet (Fig. 2a). Thus, the extrusion force can be calculated by the reaction force. The lateral surface of the billet is constrained by rigid lines to ensure the materials cannot flow along the positive direction of the radius. The coefficient of friction over this region is set to 0 which represents the zero friction

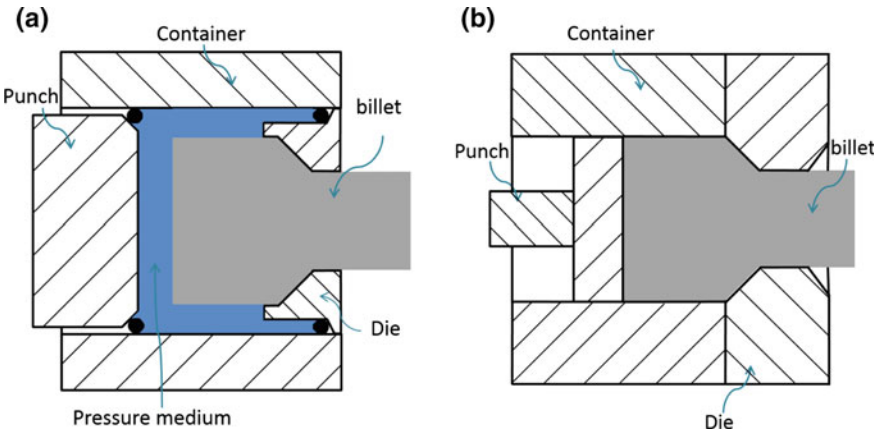

Fig. 1 Principle of **a** hydrostatic extrusion and **b** conventional extrusion

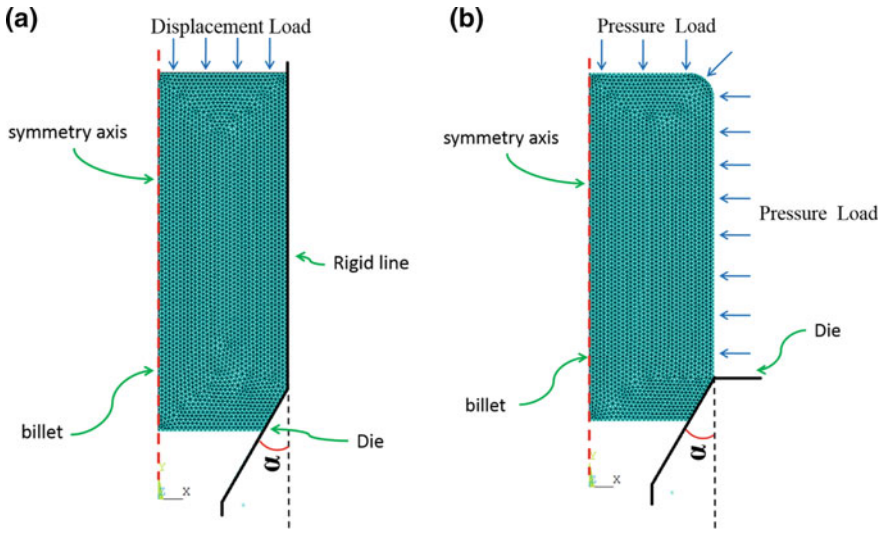

Fig. 2 Models of **a** displacement load and **b** pressure load

between billet and pressure medium. Only the rigid constraints and minimal friction coefficient cannot fully reflect all the advantages of the hydrostatic extrusion. Essentially, the displacement load model is a conventional extrusion model with near-zero friction between the billet and the die. According to the law of hydrostatic pressure, a static hydrostatic extrusion model is designed in this paper. The pressure load model is the model replacing the pressure medium as the boundary condition of the billet, modeling only its pressure properties. The pressure is set to increase linearly with the time, replacing the effect of the punch pushing the pressure medium. So, in this model, the punch is not needed because the billet is deformed by the increased pressure. In the pressure load model, the central axis of the billet is the symmetrical axis of both billet and die, and the pressure load only exists over the un-deformed outer surface of the billet (The fillet at upper right of the billet is built to verify the uniform distribution of the pressure load) [21]. Because the pressure medium used in the hot hydrostatic extrusion of pure tungsten is BN powder, so the friction coefficient is set to 0.05 [22].

A Johnson-Cook model of pure tungsten is determined by Jin et al. [23], and the equation can be described as

$$\sigma = (91.7110 + 235.8226\varepsilon^{0.2557})(1 + 0.0461\mathrm{In}\dot{\varepsilon}^{*})(1 - \mathrm{T}^{*0.5485}). \quad (1)$$

The true stress-strain curves of 1250, 1350, 1450, 1550 and 1650 °C are shown in Fig. 3. The density is 19.2 g/cm^3 and Poisson ratio is 0.28.

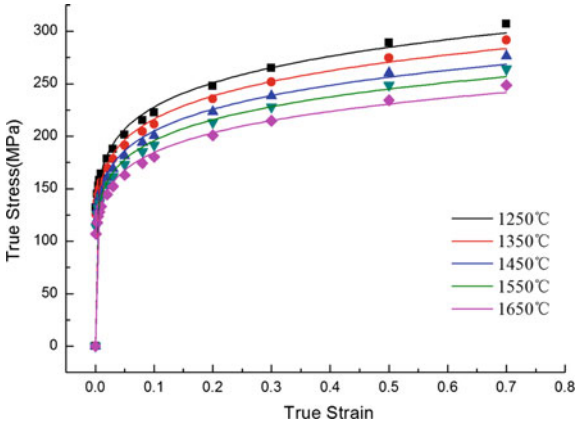

Fig. 3 True stress-strain curves under different temperature

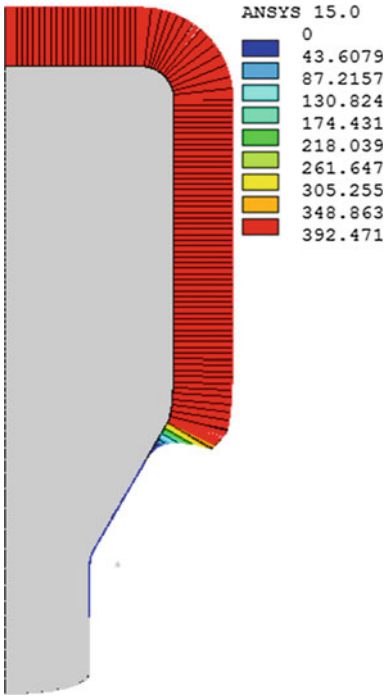

Fig. 4 Fluid pressure distribution

Finite Element Simulation Results and Discussion

The fluid pressure during the forming process can be observed in Fig. 4. Unique pressure is applied to the surface of the undeformed part and gradually decreases at the inlet zone. The existence of the hydrostatic pressure can also be confirmed by Von-Mises equivalent stress in Fig. 5. In the undeformed region, the Mises stress

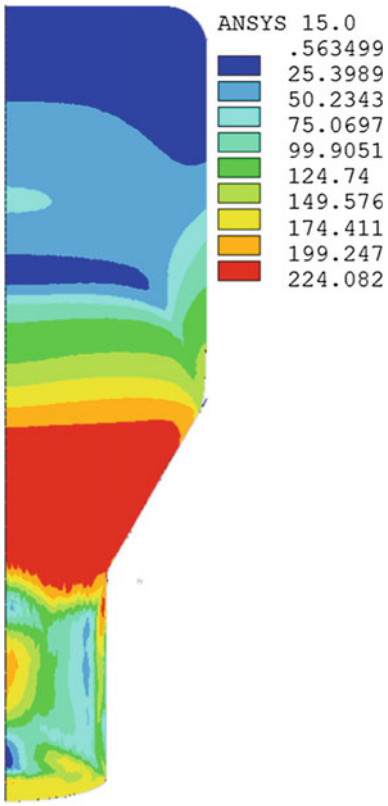

Fig. 5 Von-Mises stress distribution

value is close to zero due to the hydrostatic pressure. As the material flows to the deformation zone, the hydrostatic pressure environment disappears, the Von-Mises stress increases and the material gradually yields. The above indicates that the pressure loading method can restore the true hydrostatic extrusion process greatly.

When the half die angle $\alpha = 30°$, the region of tensile stress can be divided into 2 parts, one at the core and another at the surface (Fig. 6). Tensile stress area at the core gradually reduced when the extrusion ratio increases from 2.25 to 6.25. At the same time, under different extrusion ratios, there is a significant tensile stress distribution on the surface of the extruded part. The possible reason is, when the extrusion is relatively small, the material flow velocity at the core is slow, uneven deformation of the material leads to the existence of additional tensile stress at the central part, which is likely to cause cracks inside the material [11]. As the extrusion ratio increases, the velocity difference of the material decreases, and the additional tensile at the core gradually disappears. Meanwhile, the material flow behavior at the surface depends on the die contour shape and friction. When the extrusion ratio is too large, the friction resistance increases, the flow velocity of the material at surface is slower than that of the core. The additional tensile stress is transferred to the surface of the material, when it reaches the material tensile limit,

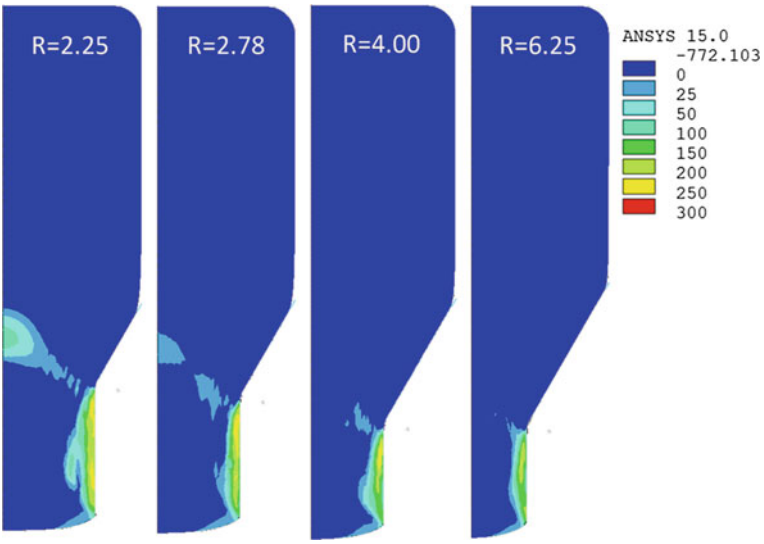

Fig. 6 Axial stress distribution under different extrusion ratios

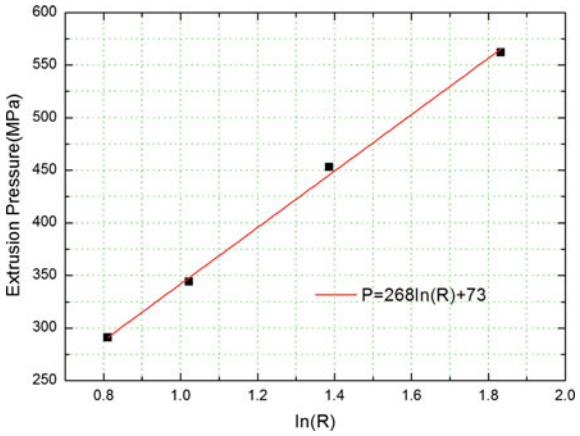

Fig. 7 Relationship between extrusion pressure (P) and extrusion ratio (R)

and then the longitudinal cracks may occur. Therefore, for the hydrostatic extrusion of pure tungsten, it is necessary to select an appropriate extrusion ratio to prevent internal and surface cracking defects.

The P value changes with the increased R and the linear relationship between P and lnR can be found as P = 268 lnR + 73 (Fig. 7), which theoretically indicates the extrusion ratio of pure tungsten can be infinite, but the R value must maintain a definite range because of material properties and device limit.

Von-Mises equivalent strain value rise as half die angle (α) respectively is 12.5°, 15°, 17.5°, 20°, 30°, 45°, 60° when R = 4.00. The large strain region extends from core to surface, a new large strain region appears near surface and expand to the

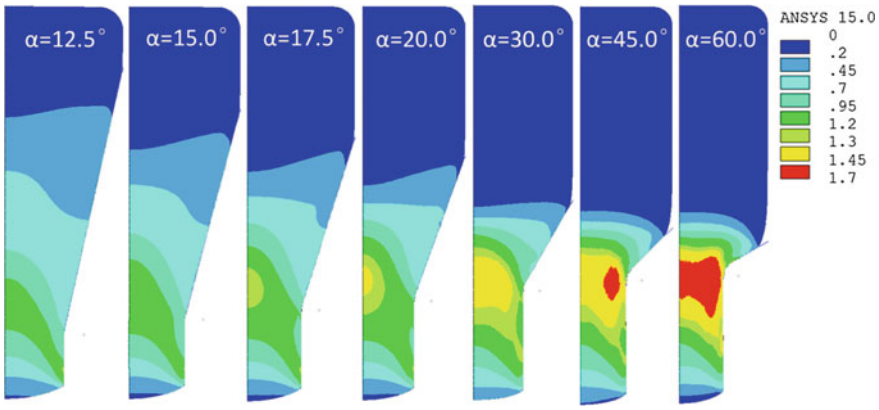

Fig. 8 Von-Mises equivalent strain under different half die angles

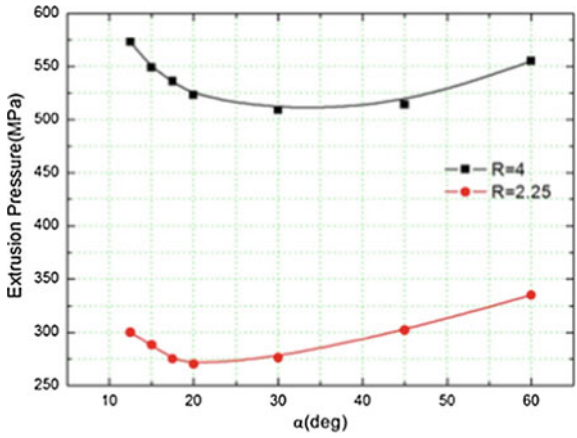

Fig. 9 Relationship between extrusion pressure (P) and half die angle (α)

core after 30° (Fig. 8). The uneven distribution of strain manifests the non-uniform deformation, and inhomogeneity intensifies after 30°.

The extrusion pressure under different angles also indicates this non-uniform deformation. P value decreases firstly then increases as α rises from 12.5° to 60°. The angle corresponding with the lowest P value is the optimal die angle, 40° when R = 2.25 and 60° when R = 4.00, respectively (Fig. 9). The magnitude of the optimal angle depends on the deformation redundant work and friction work. The redundant work is the extra work required to resist uneven deformation that rises when the die angle increases. At the same time, the change of the angle leads to the contact pressure, contact area changes, which directly affects the friction work. The two works together on the α—P relationship result in the existence of the optimal die angle. When R value changes, the redundant work, friction work is changed directly, resulting in the change of optimal angle. That is the reason why the optimal die angle is different under different extrusion ratio.

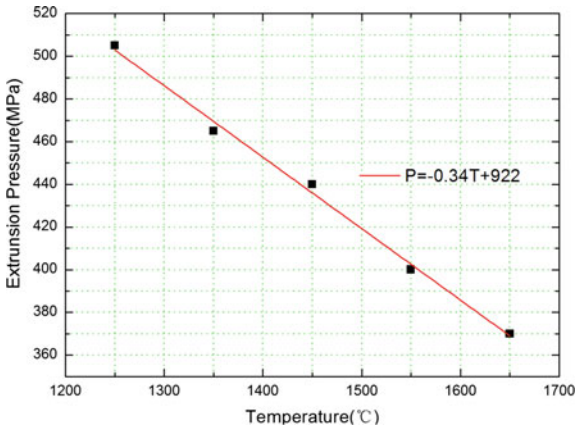

Fig. 10 Relationship between extrusion pressure (P) and temperature (T)

Figure 10 shows the effect of temperature on the extrusion force between 1250 and 1650 °C. When the half-mode angle is 30° and the extrusion ratio is 4.00, it can be found that the squeezing force P decreases linearly with the temperature T described as $P = -0.34\ T + 922$. Increasing the extrusion temperature can greatly reduce the extrusion pressure of the hydrostatic extrusion, prolong the life of the molder and complete larger deformation amount. But the high temperature will make the grain growth phenomenon more significant, which is not conducive to the refinement of tungsten grains and improvements of synthetical properties.

Experiments Results and Discussion

Based on the simulation results, the corresponding experiment of hot hydrostatic extrusion is carried out at 1550–1600 °C on the basis of practical operating conditions. The diameter of the billet is 50.0 mm (Fig. 11), the diameter of the product is 25.0 mm (Fig. 12) and the extrusion ratio is 4.00. The extruded tungsten with good surface quality can be found without any cracking defects, which proves that the simulation results have a certain guiding effect.

The microhardness on the transverse cross section of the material before and after extrusion is measured. The hardness distribution on the sintered billet is relatively uniform, as shown in Table 1. Hardness is basically same during central and edge area, about 367.83 $HV_{3.0}$. Compared to the sintered billet, the monolithic hardness of the extruded rod is significantly improved, which is due to the increasing density of dislocation caused by the deformation process. The hardness of the extruded tungsten rods shows a tendency of decrease during the radial direction (Fig. 13). The main reasons for this phenomenon can be concluded as below: uniform material flow during the extrusion process; low deformation ratio of the surface material due to the rapidly drop down of the surface temperature.

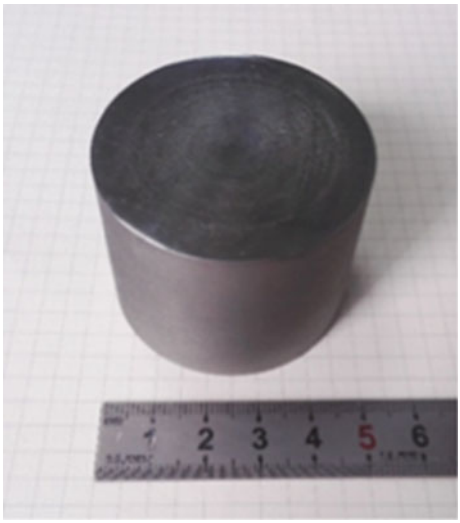

Fig. 11 Sintered tungsten billet

Fig. 12 Tungsten rod after hydrostatic extrusion

Table 1 Microhardness values of sintered tungsten billet of transverse cross section

Region	Vickers hardness ($HV_{3.0}$)					Mean ($HV_{3.0}$)
Center	364.8	376.9	364.8	378.4	361.8	369.3
Transition	372.3	370.7	361.8	368.4	368.3	367.6
Edge	370.7	372.3	360.4	366.2	363.8	366.6

The microstructure of the transverse cross section of the material before and after extrusion is observed by means of SEM (Fig. 14). The tungsten grains are greatly refined after hydrostatic extrusion. The microstructure of the extruded tungsten rod is observed during the transverse and longitudinal cross section (Fig. 15). In the transverse cross section, the grain shape is nearly circular, and the grain size is

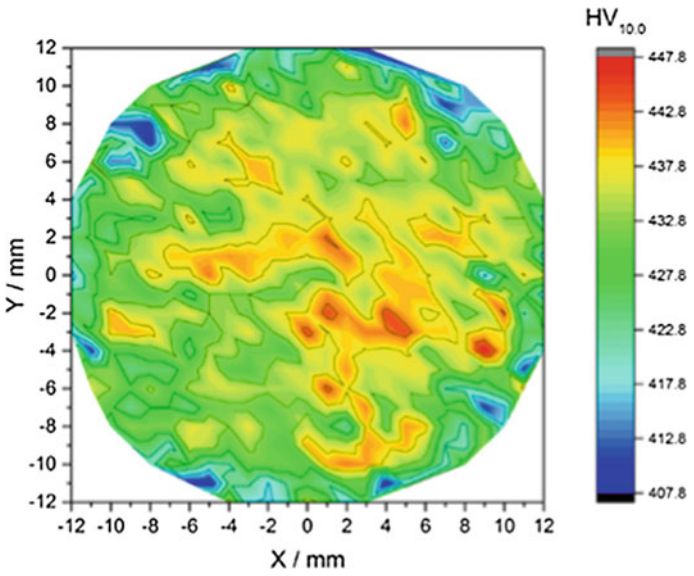

Fig. 13 Microhardness distribution of extruded rod during transverse cross section

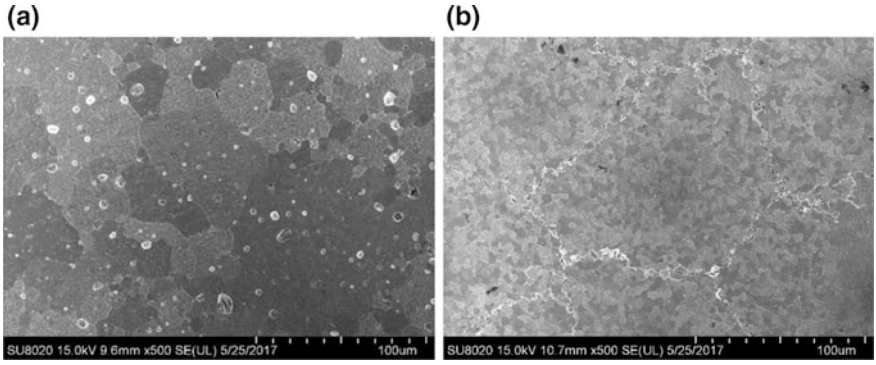

Fig. 14 Microstructure of sintered pure tungsten **a** before extrusion and **b** after extrusion

uniform. Meanwhile, its longitudinal section grain is stretched into an oval shape in the direction of the extrusion during the hydrostatic extrusion deformation.

The dynamic compression tests of sintered and hydrostatic extruded tungsten are carried out at room temperature and by means of the Hopkinson bar. The dynamic strain rate $\dot{\varepsilon} = 1200\,\mathrm{s}^{-1}$ is used and the true stress-strain curves are shown in Fig. 16. The yield strength of sintered tungsten is increased from about 1.3 GPa to the extruded 2.0 GPa. This is because tungsten grains are significantly refined during the extrusion process. Meanwhile, the hardening modulus of the material after extrusion is obviously reduced, and the work hardening phenomenon is not

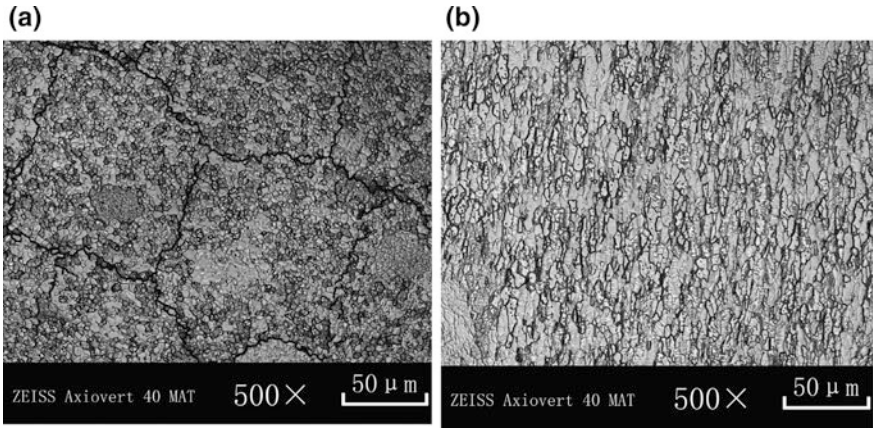

Fig. 15 Microstructure of extruded rod during **a** transverse cross section and **b** longitudinal cross section

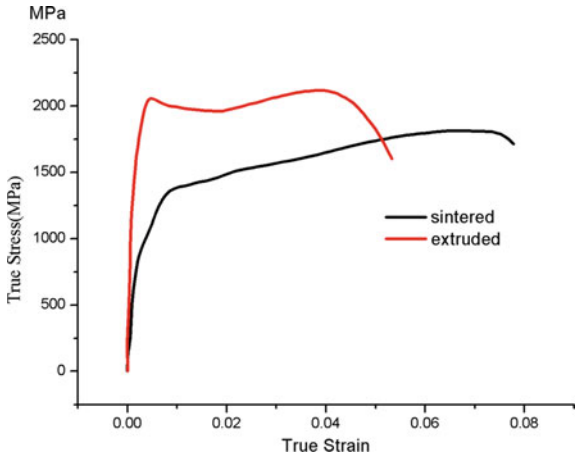

Fig. 16 True stress-strain curves of sintered billet and extruded rod

obvious. This is because during the deformation process, the dislocation density tends to saturate, and the strain hardening rate is gradually reduced. Oppositely, the initial dislocation density of the sintered tungsten is very low, so the rate of dislocation multiplication is faster than that of the dislocation recovery rate, leading to the lattice distortion energy increase, the dislocation movement is greatly resisted, the deformation resistance of the material is relatively large, the strain strengthening effect is obvious.

Summary

The hot hydrostatic extrusion process of sintered pure tungsten is studied by finite element analysis and related experiments. A finite element model of hydrostatic extrusion with hydrostatic pressure is designed. This model can better respond to the hydrostatic pressure effect compared with traditional displacement loading model. Further, the hydrostatic extrusion process under different R and α was simulated by this model during 1250–1650 °C. The results show that when the extrusion ratio R increases from 2.25 to 6.25, the tensile stress region at central region disappears gradually, meanwhile the extrusion pressure P increases, and the relationship between the P and R is P = 268 ln(R) + 73. When α increases from 12.5° to 60°, the P value first decreases and then increases. The optimal die angle is 40° when R is 2.25, 60° when R is 4.00, respectively. As temperature increases from 1250 to 1650 °C, the extrusion pressure decreases linearly. Based on the numerical simulation results, the hot hydrostatic extrusion experiment of pure tungsten is carried out. After the hydrostatic extrusion, the grain size refinement effect is obvious and the hardness is significantly improved. The dynamic compression experiment results show that the yield strength of tungsten after hydrostatic extrusion is improved from 1.3 GPa in sintered state to 2.0 GPa in extrusion state while the effect of strain hardening is weakened.

Acknowledgements This paper was supported by National Magnetic Confinement Fusion Program with Grant No. 2014GB121001 and National Natural Science Foundation of China with Grant No. 51575128.

References

1. H. Bolt, V. Barabash, G. Federici et al., Plasma facing and high heat flux materials—needs for ITER and beyond. J. Nucl. Mater. **307–311**, 43–52 (2002)
2. M. Merola, D. Loesser, A. Martin et al., ITER plasma-facing components. Fusion Eng. Des. **85**, 2312–2322 (2010)
3. V. Philipps, Tungsten as material for plasma-facing components in fusion devices. J. Nucl. Mater. **415**, S2–S9 (2011)
4. X.Y. Ding, L.M. Luo, L.M. Huang et al., Research progress in irradiation damage of tungsten and tungsten alloys for nuclear fusion reactor. Chin. J. Rare Met. **39**, 1139–1147 (2015)
5. T. Hirai, F. Escourbiac, S. Carpentier-Chouchana et al., ITER tungsten divertor design development and qualification program. Fusion Eng. Des. **88**, 1798–1801 (2013)
6. R.A. Pitts, S. Carpentier, F. Escourbiac et al., A full tungsten divertor for ITER: Physics issues and design status. J. Nucl. Mater. **438**, S48–S56 (2013)
7. M. Rieth, S.L. Dudarev, S.M.G.D. Vicente et al., Recent progress in research on tungsten materials for nuclear fusion applications in Europe. J. Nucl. Mater. **432**, 482–500 (2013)
8. F.C. Wang, *Hydrostatic Extrusion* (1st, National Defense Industry, Beijing, 2008)
9. Z.H. Zhang, F.C. Wang, S.K. Li et al., Deformation characteristics of the 93 W–4.9Ni–2.1Fe tungsten heavy alloy deformed by hydrostatic extrusion. Mater. Sci. Eng., A. **435–436**, 632–637 (2006)

10. Z.H. Zhang, F.C. Wang, Research on the deformation strengthening mechanism of a tungsten heavy alloy by hydrostatic extrusion. Int. J. Refract. Met. Hard Mater. **19**, 177–182 (2001)
11. А.Н. Колпашников, *Hot Liquid Extrusion of Metal Materials* (National Defense Industry, Beijing, 1988)
12. D.R. Li, Z.Y. Liu, Y. Yu et al., Numerical simulation of hot hydrostatic extrusion of W-40wt. % Cu. Mater. Sci. Eng., A. **499**, 118–122 (2009)
13. B. Manafi, M. Saeidi, Deformation behavior of 93 Tungsten alloy under hydrostatic extrusion. Int. J. Adv. Manuf. Technol. **76**, 28487–28492 (2014)
14. F.C. Wang, Z.H. Zhang, S.K. Li, Numerical simulation for the process of hydrostatic extrusion of 245 tungsten alloys with different die contours. Acta Armamentarii. **22**, 525–528 (2001)
15. R. Kopp, G. Barton, Finite element modeling of hydrostatic extrusion of magnesium. J. Technol. Plast. **28**, 1–12 (2003)
16. Q. Zhou, R.Q. Xu, Lubricating properties and development application of graphite materials. New Carbon Mater. 11–16 (1997)
17. J. Robertson, Method of and apparatus for forming metal articles, British Patent No. 19 356 (October 14, 1893), US Patent (1894) 504
18. H.L.D. Pugh, *The Mechanical Behaviour of Materials Under Pressure* (Elsevier, 1987), pp. 525–590
19. Z.H. Zhang, F.C. Wang, Y.M. Sun et al., Finite element analysis and experimental investigation of the hydrostatic extrusion process of deforming two-layer Cu/AI composite. J. Beijing Inst. Technol. (English Edition) **22**, 544–549 (2013)
20. A. Feuerhack, C. Binotsch, A. Wolff et al., A numerical criterion for quality prediction of bimetal strands. J. Mater. Process. Tech. **214**, 183–189 (2014)
21. S.Q. Du, X. Zan, P. Li et al., Comparison of hydrostatic extrusion between pressure-load and displacement-load models. Metals **7**, 78 (2017)
22. Q.L. Guo, The contrast between the effect of boron nitride and that of common solid lubricant additives on sliding friction. J. G Univ. Technol. (Nat Sci Ed) **26**, 41–46 (1997)
23. W. Jin, G.Q. Zhao, L. Chen et al., A comparative study of several constitutive models for powder metallurgy tungsten at elevated temperature. Mater. Des. **90**, 91–100 (2016)